Seismic Performance at Beam Ends of Unbonded Prestressed Precast Concrete Frames

Yuchen Jiang[2,a], Jian Wang[1, b], Jiabin Wen[1, c], Haoyang Shuai[3, d] and Zhijun Cheng[4, e]

[1]Jiangsu Vocational College of Agriculture and Forestry, Zhenjiang 212400, China;

[2]College of Civil Engineering, Taihu University of Wuxi, Wuxi 214064, China;

[3]Xi'an Jiaotong-liverpool University, Suzhou 215028, China.

[4]Longxin Construction Group Technology Center, Haimen 226100, China;

[a] superjyc@hotmail.com, [b] 574274138@qq.com, [c] 1113126670@qq.com, [d]940745060@qq.com, [e]1248301191@qq.com

Abstract. Numerical modelling was conducted to investigate the seismic performance at beam ends of unbonded prestressed precast concrete frames. The established finite element model was verified by the test results. Through numerical simulation, the influence of such factors as the presence or absence of energy-dissipating reinforcement, the length of the unbonded section of energy-dissipating bars, the amount of prestressed or non-prestressed reinforcement on the seismic performance at beam ends of unbonded prestressed precast concrete frames were further analyzed. The results show that all prestressed precast beam-end models have similar initial stiffness. The bearing capacity and energy-dissipating performance of beam-end models without energy-dissipating bars are the lowest. The length of the unbonded section of energy-dissipating bars has no significant effect on the bearing capacity and energy-dissipating capacity of beam-end models, though the yield displacement increases obviously with the increase of the length of the unbonded section, as the local stress of energy-dissipating bars is reduced by setting the unbonded section. The bearing capacity of beam-end models can be improved by increasing the amount of prestressed or non-prestressed reinforcement. In the case of the same amount of prestressed reinforcement, increasing the amount of energy-dissipating bars can significantly improve the energy-dissipating capacity.

Keywords: Precast concrete frames; beam end; numerical modelling; seismic performance; energy-dissipating capacity.

1. Introduction

The traditional high energy consumption, labor intensive construction mode can no longer meet the requirements of sustainable development, and it is imperative to vigorously develop prefabricated buildings and promote the industrialization of construction. There are two kinds of prefabricated concrete structures with potential applications in seismic fortification areas: assembled monolithic concrete structures and prestressed precast concrete structures. The assembled monolithic concrete structure is the most studied and the most widely used prefabricated structure at present. As a combination of precast components and cast-in-place concrete, the assembled monolithic concrete structure has similar structural performance as the monolithic concrete structure. However, wet operation on site can not be avoided, and it has the shortcomings of large residual deformation and high repair cost after earthquake. The prestressed precast concrete structure is a structural form in which the precast components are mainly connected by prestressed tendons. There are many advantages to using post-tensioned prestressing technology, such as saving construction costs, improving production efficiency, and reducing the residual deformation after earthquake. Furthermore, the damage of such structure is concentrated near the joint surface and can usually be repaired quickly after an earthquake.

As illustrated in Fig. 1, the Prestressed precast concrete frame joint is assembled by stretching the prestressed tendons. Precast concrete frame joints with unbonded prestressed tendons require

little or no repair after an earthquake, in that the prestressed tendons provide effective elastic restoring force, leading to very small residual deformation. However, the energy-dissipating capacity of the concrete frame assembled only by prestressed tendons is insufficient, and the drift ratio may quickly exceed the specified limit once the beam and column are detached. At present, mild steel bars are commonly installed in joint area to improve the energy-dissipating capacity.

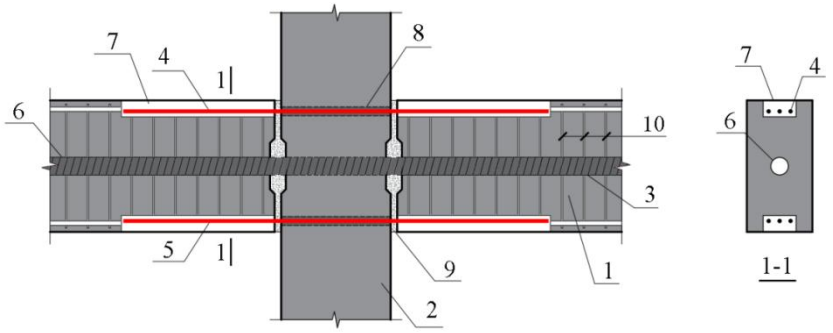

Fig. 1 Prestressed precast concrete frame joints (1 - Precast beam; 2 - Precast column; 3 - Prestressed tendons; 4 - Top energy-dissipating bars; 5 - Bottom energy-dissipating bars; 6 - Corrugated pipe; 7 - Reserved notch at the beam end; 8 - Reserved hole in the column; 9 - Grouted joint; 10 - Stirrups)

The research on prestressed precast concrete frames began in the early 1990s, mainly including the NIST project in the United States and the PRESSS project jointly carried out by the United States and Japan. In phase I to III of NIST project, prestressed assembled beam-column joints without non-prestressed reinforcement were tested, and the influences of the type, location and bonding condition of the prestressed reinforcement were analyzed. The results showed that: the bearing and deformation capacity of prestressed assembled beam-column joints could reach or even exceed that of cast-in-place joints, whereas the energy-dissipating capacity was usually insufficient. The energy-dissipating performance of the joint was improved by setting the prestressed reinforcement in the middle position of the beam height and replacing the prestressed rod with the prestressed strands. By using unbonded or partially bonded prestressed tendons, the prestressed tendons always remain elastic, thus reducing the residual deformation and improving the self-reset performance [1, 2]. In phase IV of NIST project, experimental studies were conducted on hybrid-connected beam-column joints with energy-dissipating bars, and the results showed that the seismic performance of hybrid-connected joints was equal to or better than that of cast-in-place joints [3]. Phase I of PRESSS project mainly focused on precast prefabricated concrete structural systems with potential applications in earthquake areas, and discussed the feasibility of the post-tensioned prestressing technology [4, 5]. Subsequently, experimental and theoretical studies on the seismic performance of beam-column joints were carried out in Phase Ⅱ of PRESSS [6]. In Phase III of PRESSS project, the scale model test on a five-layer prefabricated frame was carried out. Four different joint connection types, including hybrid connection, prestressed connection and two kinds of non-prestressed connections, were adopted in the frame model. The results showed that the prestressed precast concrete frame with hybrid connection had good seismic performance and could be applied in high intensity area [7].

In addition to the NIST project and the PRESSS project, there are many other studies focused on the seismic performance of prestressed precast concrete frames [8-12]. Ozden and Ertas [8] investigated the influence of non-prestressed reinforcement contend on the seismic performance of the post-tensioned precast concrete specimens by experiments, and concluded that a 20%-30% non-prestressed reinforcement contribution to the flexural strength seemed to be the most rational connection design, if adequate strength, ductility, relative energy dissipation ratio, and minimum permanent displacement criteria were considered. Morgen and Kurama [9], Rodgers et al. [10-12] proposed to use external damping device in the joint region instead of energy-dissipating

reinforcement to improve the seismic performance, and it was found that the seismic performance of the joints with external damping device was equal to or even better than that of hybrid joints.

However, the solution of external damping device in the joint area will significantly increase the construction cost, but also put forward higher requirements on the fabrication and installation precision of prefabricated components. In consideration of structural performance and economic benefits, it is more feasible to improve the energy-dissipating capacity of the joint by built-in energy-dissipating reinforcement. To provide experimental basis and theoretical support for the research and application of this kind of structure, it is necessary to further analyze and confirm the influence of such factors as the length of the unbonded section of energy-dissipating bars, the amount of prestressed or non-prestressed reinforcement on the seismic performance of prestressed precast concrete frame joints.

As part of the overall research plan, this paper focuses on the finite element analysis of beam-end specimens, aiming to provide reference for the parameter design of specimens in the subsequent experimental studies. It should be noted that a low-cycle reciprocating loading test has been carried out on a beam-end specimen (No. PNS3 in Table 1), and the test results can be used to verify and modify the finite element model in the present study.

2. Model establishment

2.1 Dimension and reinforcement configuration

The dimension and reinforcement configuration of beam-end specimens for the numerical simulation in the present paper are illustrated in Table 1 and Fig. 2. Specimens PNS1 and PNS2 are unbonded prestressed precast beam-end specimens without energy-dissipating bars. Specimens PNS3~9 are unbonded prestressed precast beam-end specimens with energy-dissipating bars, among which the varying parameters are the length of the unbonded section of energy-dissipating bars and the amount of prestressed or non-prestressed reinforcement. In all beam-end specimens, the prestressed strands are located in the middle position of the beam height. Low shrinkage cement-based material with 1% copper-coated steel fiber is adopted as the grouting material for the beam-base joints.

In the production process of prefabricated members, corrugated pipes need to be reserved for the prestressed steel strands and energy-dissipating steel bars. A steel cage with a bar diameter of 22 mm is arranged in the base member to ensure sufficient stiffness and strength relative to the beam member.

Table 1. Reinforcement configuration

Specimen No.	Energy-dissipating bars	Beam bars	Prestressed strands	Beam stirrups	Unbonded section length
PNS1	——	2C10	3UA^{s}15.2	C8@100/150(2)	——
PNS2	——	2C10	5UA^{s}15.2	C8@100/150(2)	——
PNS3	2C18	2C18	3UA^{s}15.2	C8@100/150(2)	——
PNS4	2C18	2C18	5UA^{s}15.2	C8@100/150(2)	——
PNS5	2C18	2C18	5UA^{s}15.2	C8@100/150(2)	50 mm
PNS6	2C18	2C18	5UA^{s}15.2	C8@100/150(2)	150 mm
PNS7	2C22	2C22	5UA^{s}15.2	C8@100/150(2)	——
PNS8	2C22	2C22	5UA^{s}15.2	C8@100/150(2)	50 mm
PNS9	2C22	2C22	5UA^{s}15.2	C8@100/150(2)	150 mm

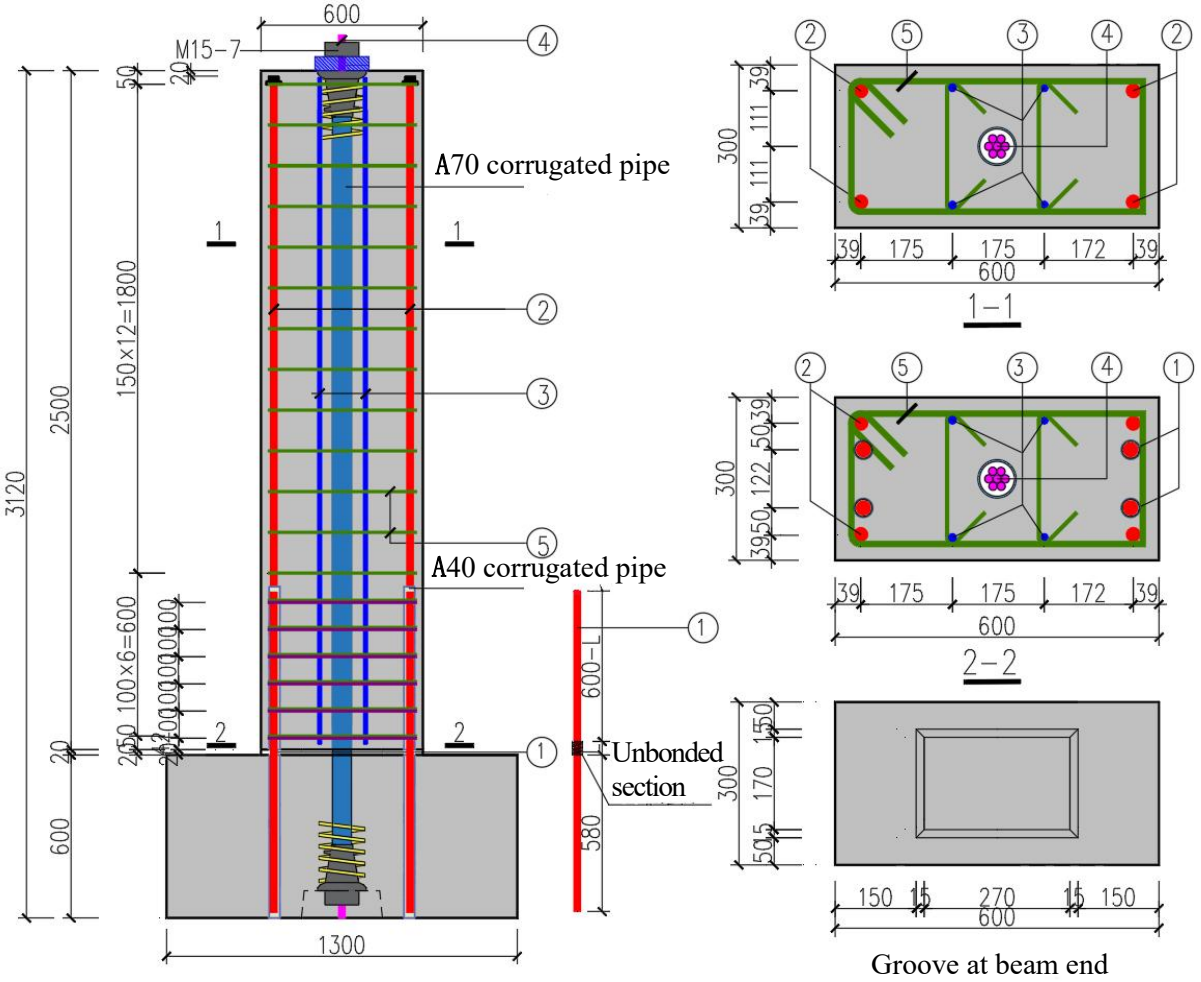

Fig. 2 Dimension and reinforcement arrangement

2.2 Element type and material constitutive model

Three-dimensional eight-node elements with reduced integration (C3D8R) are used in the simulation of concrete beams, concrete bases, grout joints and steel plates. Two-node linear three-dimensional truss elements (T3D2) are used to simulate longitudinal bars, stirrups and prestressed strands. The Concrete Damaged Plasticity (CDP) model is employed to model the mechanical properties of concrete. The CDP model takes into account the damage caused by tension or compression, and can also reflect the degradation of stiffness. The uniaxial compression stress-strain relation of concrete is determined according to GB 50010-2010 [13], and the tensile behavior of concrete is assumed to increase linearly up to the tensile strength. The tension stiffening option is adopted to define the mechanical behavior of concrete after cracking. The tensile stress of concrete decreases linearly to zero at the strain of 0.05. The stress-strain curve of concrete is shown in Fig. 3a. The longitudinal reinforcement and stirrups adopt an ideal elastic-plastic model, which assuming that the strength of the steel will not change after reaching the yield strength (Fig. 3b). The prestressed strands and the copper-coated steel fiber cement-based composites are defined as linear elastic materials. The mechanical properties of reinforcement, concrete and grouting material obtained from preliminary material tests are shown in Table 2 and Table 3 respectively.

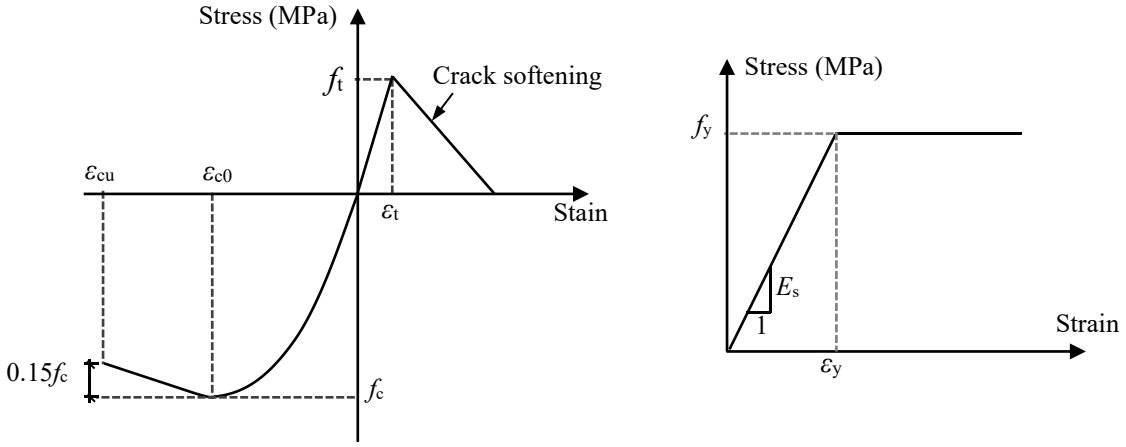

(a) Concrete (b) Steel

Fig. 3 Stress-strain law for concrete and steel in the FE model

Table 2. Mechanical properties of reinforcement

	Yield Strength/MPa	Tensile strength/MPa	Elastic modulus/GPa
C10	425	610	203.3
C18	423	620	201.6
C22	428	600	205.1
A^s15.2	423	620	201.6

Table 3. Mechanical properties of concrete and grouting material

	Compressive strength/MPa	Elastic modulus/MPa
Concrete-beam	36.8	36251
Concrte-base	36.3	34177
Grouting material	92.4	36925

2.3 Presstressing and contact

Beam and base members are modeled separately, with the tangential behavior of the beam-base contact surface defined as "Penalty", and the friction coefficient is set as 0.6. The normal behavior is set to "Hard Contact". There may exist slip between reinforcement and concrete, but if all slippage is considered, the calculation amount is too large, resulting in convergence problems. As a result, only the slip between the energy-dissipating bars and the concrete is considered, and the rest reinforcement bars adopt "Embedded Region" contact setting option. The slip between reinforcement and concrete is simulated by "SPRING2" nonlinear spring elements. The parameters of the nonlinear spring are determined according to the bond-slip constitutive model in GB 50010-2010 [13].

The prestress is applied by reducing temperature in the simulation, and the cooling temperature can be calculated as:

$$\Delta T = \frac{\sigma}{\alpha E_s}$$

where ΔT, σ and E_s are the cooling temperature, initial stress and elastic modulus of the prestressed strands, respectively; α is the temperature linear expansion coefficient of concrete, which can be taken as 1.2×10^{-5}.

In the finite element model, MPC-BEAM contact is adopted between the two ends of the strand and the center of the steel plates (simulated the anchors), so that the prestress can be concentrated

on the steel plate. The nonlinear finite element model established according to the test specimen is shown in Fig. 4.

In ABAQUS software, there are three analysis steps: first, the initial step; second, the step of applying prestress, in which the prestress is generated form the temperature difference between this step and the initial analysis step; third, the step of displacement loading.

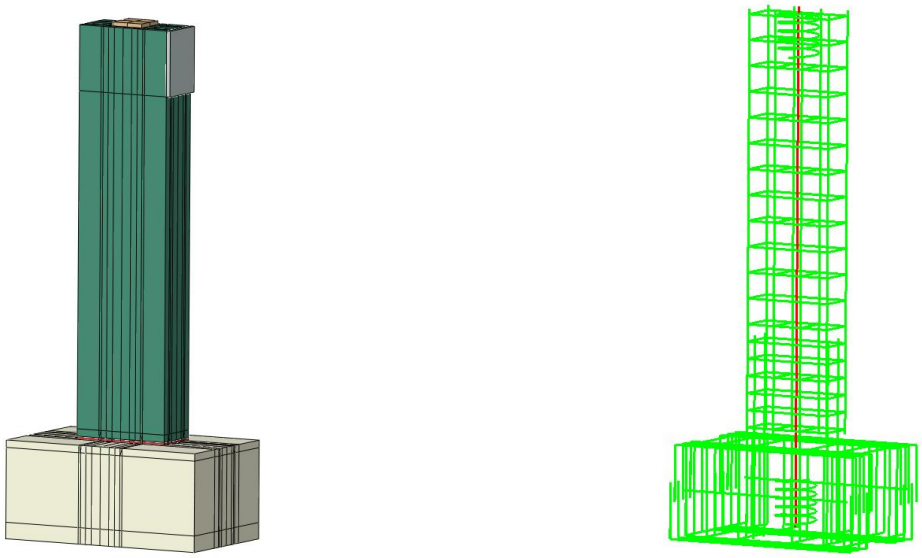

(a) Beam and Base (b) Reinforcement and prestressed strands

Fig. 4 Finite element model of prestressed precast beam-end specimen

3. Validation

The simulated stress nephogram of reinforcement and damage nephogram of concrete at 3.5% drift ratio are shown in Fig. 5a~c, respectively. The simulated failure mode is highly consistent with the test failure mode, as the concrete compression damage is concentrated in the corner area of the beam end, and the tensile damage mainly appears in the lower 1/3 height of the beam. The energy-dissipating bars have yielded in a range near the joint surface, while the longitudinal bars in the prefabricated beams haven't yielded.

The comparison between simulated and experimental hysteretic curves of specimen PNS3 is shown in Fig. 6. It can be seen that finite element modelling well predicts the bearing capacity of the beam-end specimen and also reflects the pinching effect of the prestressed member. The simulated initial stiffness is close to the test value in the negative direction, but exceeds 40% of the test value in the positive direction. This is because the finite element modeling adopts ideal boundary conditions, without considering the influence of the elasticity and clearance of the anchor and test device. There are also differences between the material constitutive models and the actual material properties. In addition, the simulated hysteretic curve is symmetrical in the positive and negative directions, while the experimental hysteretic curve has obvious deviation in two directions, which further indicates that the experimental error is uncertain.

4. Parameter analysis

Based on the established finite element model, the low-cycle reciprocating loading tests of specimens PNS1~9 were simulated, and the influences of factors such as the existence of energy-dissipating steel bars, the length of the unbonded section of energy-dissipating steel bars, the amount of prestressed or non-prestressed reinforcement on the seismic performance at beam ends of unbonded prestressed concrete frames were further analyzed. Skeleton curves and energy-dissipating curves of specimens PNS1~9 are shown in Fig. 7 and Fig. 8 respectively. It can be seen that all prestressed precast beam-end models have similar initial stiffness. The bearing

capacity and energy-dissipating performance of beam-end models without energy-dissipating bars are the lowest. The length of the unbonded section of the energy-dissipating bars has no significant effect on the bearing capacity and energy-dissipating capacity, though the yielding displacement of beam-end specimens increases obviously with the increase of the length of the unbonded section, which is attributed to the fact that the unbonded section reduces the local stress of the energy-dissipating bars. The bearing capacity of beam-end specimens can be improved by increasing the amount of both the prestressed and non-prestressed reinforcement. With the same amount of prestressed reinforcement, increasing the amount of energy-dissipating reinforcement can significantly improve the energy-dissipating capacity.

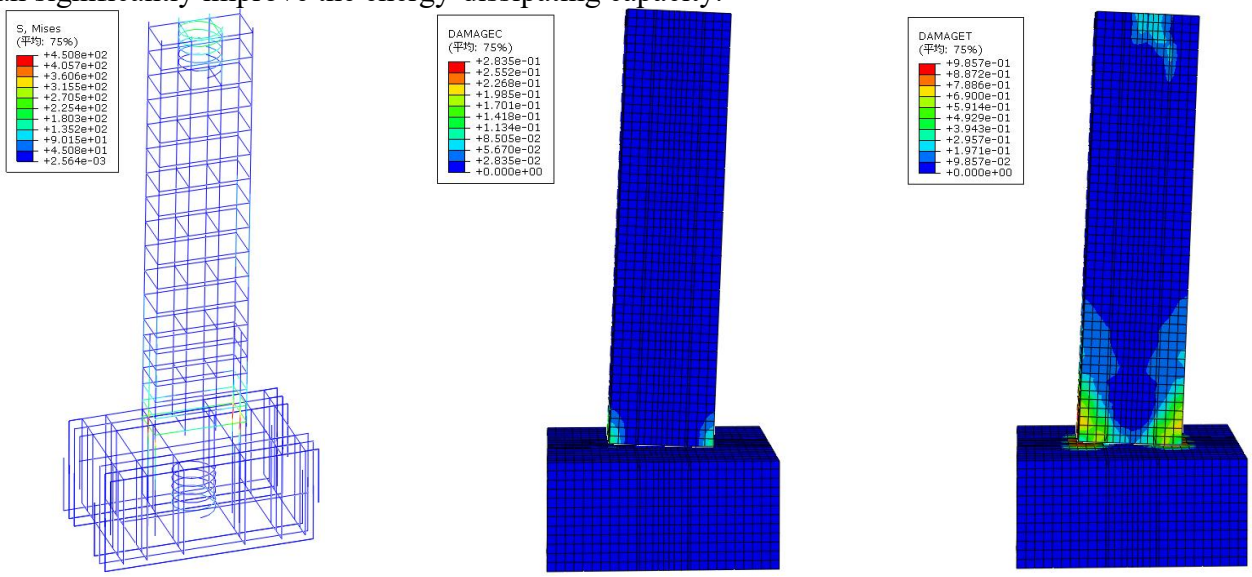

(a) Stress of reinforcement (b) Concrete compressive damage (c) Concrete tensile damage

Fig. 5 Results of Finite element modelling

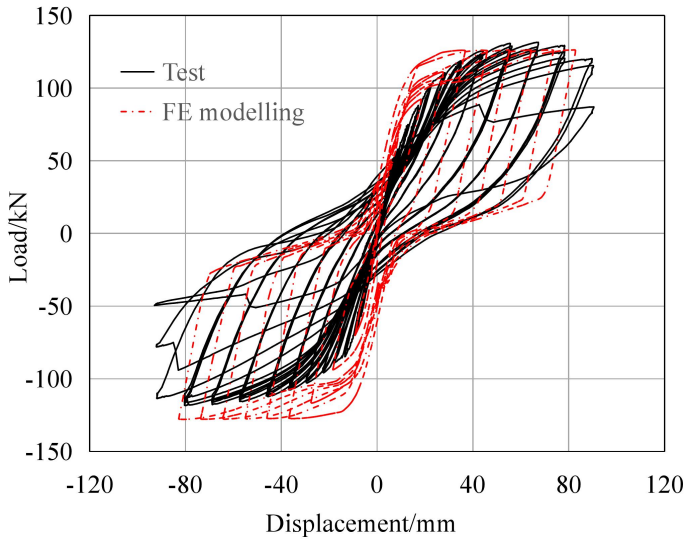

Fig. 6 Comparison of hysteresis curves between finite element modelling and test

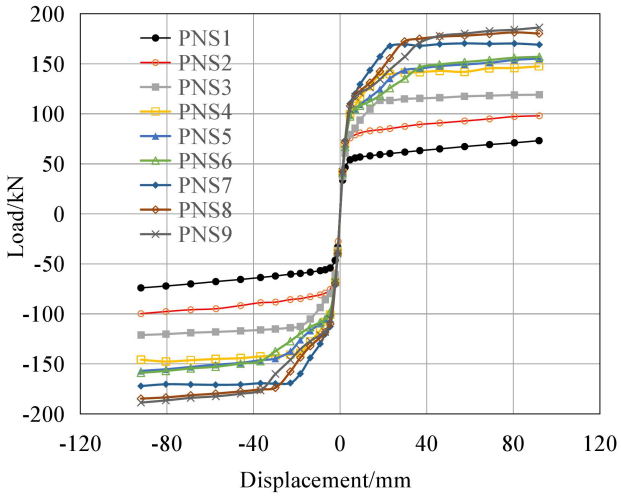

Fig. 7 Skeleton curves from finite element modelling

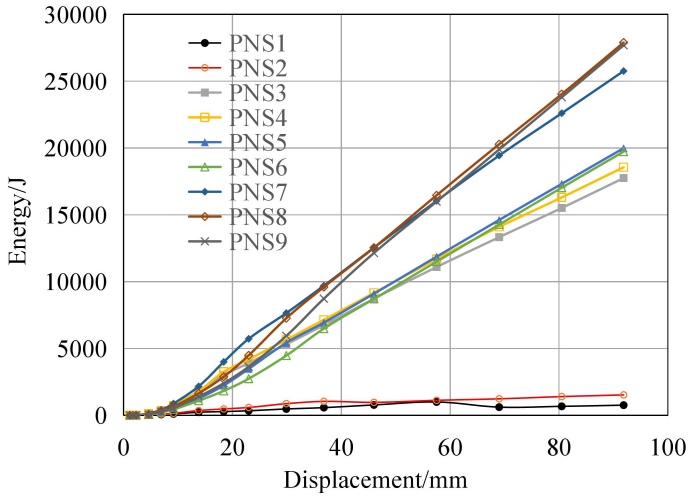

Fig. 8 Energy dissipation curves from finite element modelling

5. Summary

In this paper, the seismic performance at beam ends of unbonded prestressed precast concrete frames was investigated by numerical modelling. With the validated finite element model, some key parameters affecting the seismic performance of unbonded prestressed precast concrete joints were analyzed and discussed. The main conclusions can be drawn as follows:

(1) Numerical modelling based on ABAQUS software well predicts the bearing capacity of the beam-end specimens and reflects the pinching effect of the prestressed member.

(2) The length of the unbonded section of energy-dissipating bars has no significant effect on the bearing capacity and energy-dissipating capacity of beam-end models.

(3) The bearing capacity of beam-end models can be improved by increasing the amount of prestressed or non-prestressed reinforcement. In the case of the same amount of prestressed reinforcement, increasing the amount of energy-dissipating bars can significantly improve the energy-dissipating capacity.

Acknowledgments

The research was supported by the Natural Science Foundation of Universities in Jiangsu Province, China (No. 22KJD560006), and the 2021 Science and Technology Project of Jiangsu Vocational College of Agriculture and Forestry, China (No. 2021KJ69).

References

[1] Cheok G, Stone W, Lew H S. Partially Prestressed and Debonded Precast Concrete Beam-Column Joints[C]//Proceedings of the 3rd Meeting of the US-Japan Joint Technology Coordinating Committee on Precast Seismic Structural Systems. 1992.

[2] Cheok G S, Lew H S. Model precast concrete beam-to-column connections subject to cyclic loading[J]. PCI journal, 1993, 38(4): 80-92.

[3] Stone W C, Cheok G S, Stanton J F. Performance of hybrid moment-resisting precast beam-column concrete connections subjected to cyclic loading[J]. Structural Journal, 1995, 92(2): 229-249.

[4] Priestley M J N. Overview of PRESSS research program[J]. PCI Journal, 1991, 36(4): 50-57.

[5] Nakaki S D, Englekirk R E. PRESSS industry seismic workshops: Concept development[J]. PCI Journal, 1991, 36(5): 54-61.

[6] Priestley M J N, Tao J R. Seismic response of precast prestressed concrete frames with partially debonded tendons[J]. PCI journal, 1993, 38(1): 58-69.

[7] Priestley M J N, Sritharan S, Conley J R, et al. Preliminary results and conclusions from the PRESSS five-story precast concrete test building[J]. PCI journal, 1999, 44(6): 42-67.

[8] Ertas O, Ozden S. Behavior of unbonded, post-tensioned, precast concrete connections with different percentages of mild steel reinforcement[J]. PCI journal, 2006, 52(2): 32-44.

[9] Morgen B G, Kurama Y C. Seismic response evaluation of posttensioned precast concrete frames with friction dampers[J]. Journal of Structural Engineering, 2008, 134(1): 132-145.

[10] Rodgers G W, Solberg K M, Chase J G, et al. Performance of a damage‐protected beam‐column subassembly utilizing external HF2V energy dissipation devices[J]. Earthquake Engineering & Structural Dynamics, 2008, 37(13): 1549-1564.

[11] Rodgers G W, Mander J B, Geoffrey Chase J. Modeling cyclic loading behavior of jointed precast concrete connections including effects of friction, tendon yielding and dampers[J]. Earthquake engineering & structural dynamics, 2012, 41(15): 2215-2233.

[12] Rodgers G W, Mander J B, Chase J G, et al. Beyond ductility: parametric testing of a jointed rocking beam-column connection designed for damage avoidance[J]. Journal of Structural Engineering, 2016, 142(8): C4015006.

[13] GB 50010-2010. Code for design of concrete structures[S]. Standardization Administration of China: Beijing, China, 2010.